Food Hydrocolloids 140 (2023) 108611

Contents lists available at ScienceDirect

Food Hydrocolloids

journal homepage: www.elsevier.com/locate/foodhyd

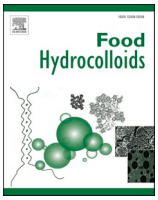

Tuning the pea protein gel network to mimic the heterogenous microstructure of animal protein

Yong Wang, Woojoeng Kim, Rishi Ravindra Naik, Patrick T. Spicer, Cordelia Selomulya *

School of Chemical Engineering, UNSW, Sydney, NSW, 2052, Australia

ARTICLE INFO

Keywords:
Curdlan gum
Pea protein
Thermal-irreversible gel
Food rheology
Large amplitude oscillation shear
Heterogenous texture

ABSTRACT

Non-extrusion texturization technology is essential to broaden the application of alternative proteins to advance sustainability and address the challenges of climate change. We propose a gelation technique to texturize non/low-gelling plant protein using curdlan gum, and to manipulate the gel texture by controlling thermal history. Pea protein and curdlan gum can form soft gel at 55–60 °C, but will form rigid gel at 80 °C. Isothermal incubation for up to 1 h could further develop the gel network with significantly higher storage modulus (e.g. 1.3 kPa without incubation, 288 kPa with 1-h incubation at 80 °C). Although curdlan-pea protein gels formed at 55–60 and 80 °C showed similar modulus ranges after 1-h incubation, the microstructure is noticeably different under microscopes (optical, CLSM, SEM). At 60 °C, large pea protein particles are still visible and only partially embedded into the curdlan network; at 80 °C, smaller protein particles are fully embedded into the gel network. When protein concentration increased from 4% to 8% w/w, the gel network became less organised as more space was occupied by protein particles. We demonstrated that heterogenous structures could be achieved by controlling the thermal history of curdlan-pea protein gels to mimic animal tissue with different stiffness (modulus) between the layers. This gelation technique can potentially be applied to other plant-sourced or alternative proteins without the need of an extruder.

1. Introduction

Plant-based food is considered a promising solution to advance sustainability and tackle climate change (Poore & Nemecek, 2019; von Braun, Afsana, Fresco, & Hassan, 2021). The EAT-Lancet Commission (Willett et al., 2019) presented the global consensus on a healthy diet and recommended that caloric intake from peas and beans (172 kcal/-day) should be five times more than that from red meat (30 kcal/day) till 2050. There are fundamental research questions for the development of disruptive products in the fast-moving consumer goods sector to replace traditional meat and dairy products, including how to better utilise plant proteins for food texturization (Ye, Georges, & Selomulya, 2018) and how other ingredients in food interact with plant proteins (Kim, Wang, & Selomulya, 2020).

Traditionally, extrusion technology has dominated the texturization of plant protein to produce the fibrous structure mimicking red meats (e.g. beef, pork). High temperature/pressure in extrusion can cause nutrient and flavour losses (Prabha et al., 2021), and often result in products with similar textures which limit the flexibility for formulation and texture adjustment. Although plant protein assemblies may reversibly be arranged into functional and often hierarchical architectures through noncovalent interactions (Freeman et al., 2018), only a few plant proteins are suitable for extrusion in commercial production. While extrusion has been successfully used for soy protein and gluten, it is still a challenge for others, including pea protein, to create fibrous or heterogenous structure via extrusion unless fortified with other proteins (Schreuders et al., 2021a) or polysaccharides (Q. L. Chen, Zhang, Zhang, Meng, & Wang, 2021). Therefore, development of an alternative approach to texturize plant proteins could unlock the potential of proteins from other varieties of plants (Sha & Xiong, 2020). Gelling technology can mimic both homogenous (i.e. egg & cheese) and heterogenous structures (e.g. seafood) using mild heating to maximize nutrient/flavour retention. Recent progress on controlled gelling to mimic human tissue scaffolding can lead to new solutions in plant-based food manufacturing (van Oosten et al., 2019), while controlled gelling can also mimic intercellular connections of animal muscle and resist external stresses (Seo et al., 2020), which have yet to be reported in food gels.

* Corresponding author.
E-mail address: cordelia.selomulya@unsw.edu.au (C. Selomulya).

https://doi.org/10.1016/j.foodhyd.2023.108611
Received 12 September 2022; Received in revised form 14 December 2022; Accepted 20 February 2023
Available online 22 February 2023

Curdlan gum is beta-glucan produced from microbial fermentation, with a high molecular weight that is made up entirely of monomeric glucose molecules connected by β-1,3-glycosidic bonds (P. Yu, Zhou, & Yang, 2019). Curdlan has been approved as food stabiliser or emulsifier by US FDA, and can perform as dietary fibre in the human diet (Verma et al., 2020). Curdlan aqueous dispersion has unique gel formation behaviours, which can form either a thermo-reversible or thermo-irreversible gel under different heating conditions (Nishinari, Zhang, & Funami, 2021). This is because curdlan assumes a triple-helical structure in which one β-1,3-glucan chain forms inter-strand hydrogen bonds with two other strands perpendicular to the axis of the triple helix (Cai & Zhang, 2017). Curdlan gum has been used to modify the gel structure of both animal and plant proteins, including pork myofibrillar protein, fish surimi, sausage, whey protein, and soy protein isolate (Florczuk, Dąbrowska, & Aljewicz, 2022; S. Jiang, Cao, Xia, Liu, & Kong, 2019; M. Li et al., 2022a; Q. Li, Wang, Miao, Zhang, & Zheng, 2019; Mi et al., 2021a; Wei et al., 2018; Wu et al., 2015; Zhao, Chen, Hemar, & Cui, 2020). However, all these proteins can form the skeleton in the gel themselves without curdlan addition, and curdlan gum only functions as the structure modifier with relatively low concentrations compared to the protein.

The significance of this study is in the development of a new approach to develop different structures using thermally controllable gelation instead of extrusion. Pea protein isolate (PPI) was selected as it is popular in the plant protein products sector considering its low-odour and low-allergenic nature. As pea protein only forms weak gels by itself (Tanger, Müller, Andlinger, & Kulozik, 2022), many methodologies have been attempted to improve the gelling property of pea protein, including cold plasma (S. Zhang, Huang, Feizollahi, Roopesh, & Chen, 2021), high-pressure processing (Sim, Karwe, & Moraru, 2019), enzyme treatment (D. Chen & Campanella, 2022), or specially designed extraction and fractionation procedures (Kornet et al., 2021; Yang, Zamani, Liang, & Chen, 2021). In the current study, the hybrid gelling of polysaccharide-protein enabled the construction of a stable backbone followed by a firm gel to incorporate untreated pea protein. Food rheology was used to analyse the deformation of gels and monitor the gelation process (Qu, Wang, Li, & Wang, 2021; Yu et al., 2022). Large amplitude oscillatory shear (LAOS) rheology was also used in the characterisation of structure formations and changes in thermal transitions (Wang & Selomulya, 2022). Morphology of the gels and the microstructure were compared under optical, confocal laser scanning, and scanning electron microscopes. The current approach requires less gelation of plant proteins, compared to the traditional approach of structuring plant proteins, as here, the roles of plant proteins are as particles rather than as forming agents for the gels. This will significantly expand the application of different plant proteins, as it remains challenging to convert plant proteins into gelling agents without chemical modifications.

2. Materials and methods

2.1. Materials

Pea protein isolate was kindly provided by Roquette (Nutralys® S85 XF extra fine pea protein, CAS No 90082-41-0, France) with 84% protein concentration. Curdlan gum powder was purchased from Opal Biotech (CAS No 54724-00-4, Zhengzhou, China) with 92% w/w curdlan concentration and 3.12% w/w ash. Milli-Q water was used in all sample preparations in this study.

2.2. Sample preparation

In the analysis of gelling behaviour at different temperatures, 4% w/w curdlan gum - 4% w/w pea protein isolate suspension was used (labelled as C4P4). Typically, 8 g of curdlan gum was dry mixed with 8 g of pea protein isolate, and then added with 184 g of Milli-Q water. All curdlan gum and pea protein samples were mixed with water for 10 min at room temperature (22 ± 1 °C) using magnetic stirrer (IKA RCT magnetic hotplate, IKA, Germany), and then stored in fridge at 4 °C overnight to ensure full hydration. Samples were prepared in similar manner when analysing the effect of pea protein concentration, with pea protein concentrations of 0%, 2%, 4%, 6%, and 8% (labelled as C4P0, C4P2, C4P4, C4P6, and C4P8). The pea protein sample (4% w/w, C0P4) was prepared in the same way without curdlan gum addition.

To prepare the gels, glass bottles were filled with curdlan, pea protein, and mixed suspensions to approximately half of the height of bottle, sealed, and cooked in water bath at 50–80 °C for 5 min or 60 min, respectively. The bottles were cooled down with ice bath after heating, and kept in fridge before further analysis.

2.3. Rheological measurement

All rheological data shown in this study was performed with a strain-controlled rheometer TA ARES G2 (TA Instruments, New Castle, US), and the temperature was monitored and controlled by the Advanced Peltier System (APS). Curdlan-pea protein suspensions were loaded to the lower geometry and gelled in situ. Crosshatched steel plate geometries (both upper and lower, 40 mm diameter) were used to eliminate wall slip. To minimise the evaporation, all samples were covered by a thin layer of silicon oil, and the geometry was covered by solvent trap cap. The results were collected using TA TRIOS software version 5.1.1.

2.3.1. Gelling behaviours

Two different heating patterns were used to evaluate the gelling behaviour of gels. First, curdlan-pea protein suspensions were equilibrated at 25 °C, heated up to 50 °C, 55 °C, 60 °C, 70 °C, and 80 °C to form gels, then equilibrated at the same temperature for 60 min, and followed by cooling down to 25 °C. Both the heating and cooling rates are set as 5 °C/min. Secondly, the curdlan-pea protein suspensions were subjected to heating-cooling circles of 25-60-25-60-25 °C or 25-60-25-80-25 °C, to form thermal reversible (60 °C) and thermal irreversible (80 °C) gels, respectively.

2.3.2. Gel strength under large amplitude oscillation

Two modes (correlation and transient) were performed separately for each sample to get the rheological information in Medium (MAOS) and Large Amplitude Oscillation Shear (LAOS). The oscillation strain was set from 0.01% to 1000% with 10 data points per decade, with excitation frequencies of 1 Hz. The 2nd, 3rd, 5th, 7th, and 9th harmonics (including higher harmonic intensity, elastic and viscous Chebyshev decompositions) were calculated using TA TRIOS software with Large Amplitude Oscillatory Shear and Fourier Transform (FT) Rheology Analysis Software package. The elastic and viscous Lissajous curves were plotted using the MITlaos program (Version 2.2 beta, freeware distributed from MIT-laos@mit.edu).

2.4. Morphology

Optical microscope (Model Ci-L, Nikon, Japan) and Confocal Laser Scanning Microscope (CLSM, Zeiss LSM 800, Jena, Germany) were used to observe the structure before and after gelation. Curdlan-pea protein suspensions were loaded on the microscope glass slides and then covered by micro cover glass. The microscope slides were then heated on top of the Peltier heater (TA Instruments, New Castle, US) for 3 min at 50 °C, 55 °C, 60 °C, 70 °C, 80 °C, respectively. For CLSM, the pea protein and curdlan gum in suspensions were dyed with Nile blue A. Images were obtained using 10 × /20 × objective lens by exciting at 633 nm.

The surface morphology of gels was acquired by scanning electron microscope (SEM) analysis following previous methods with minor modifications (Tao et al., 2021). The prepared gels were rapidly quenched with liquid nitrogen, cut into 3 cubes of approximately 5 mm on each side, and then freeze-dried to obtain the SEM samples. The dried

gels were fixed on the sample holder with conductive double-sided adhesive tape, the excess dust caused by sample loading was blown off, and was coated with platinum by spraying over the surface of samples under vacuum environment (Emitech K575x Pt sputter coater). Then morphology of samples was observed at different magnifications using the scanning electron microscope (TESCAN Vega3) at 15 kV.

Fractal analysis was used to quantify the complexity of the microstructure as indicator of the network-forming to support the observation of microscopy, including box-counting theory for microscopy using ImageJ (version 1.53, National Institutes of Health, USA) (Tang, Lei, Wang, Li, & Wang, 2021).

2.5. FT-IR of protein secondary structure after thermal treatment

The Fourier-transform infrared (FT-IR) spectra of the dried gels prepared in section 2.4 were obtained using a FT-NIR/IR spectrometer (Bruker IFS66/S, Billerica, USA) in the wavelength range of 4000-400 cm^{-1} by the acquisition of 32 scans at a resolution of 4 cm^{-1}. The protein secondary structure derivatives were determined by Gaussian curve fitting of the amide I band from 1700 to 1600 cm^{-1} in the FT-IR spectra after Fourier self-deconvolution for the baseline correction using OriginPro software (version 2019b, OriginLab Corporation, Northampton, MA, USA).

2.6. Molecular docking to predict curdlan-pea protein interactions

The prediction of the docking site (blind docking) of curdlan on the subfractions of pea protein was carried out using CB-Dock 2 (Y. Liu et al., 2022) and re-verified using Autodock Qvina (Alhossary, Handoko, Mu, & Kwoh, 2015). Briefly, the protein structures (.pdb format) of the major subfractions of pea protein, namely, vicilin (7U1L), convicilin (7U1J), prolegumin (3KSC) and curdlan (CHEBI 37671), were downloaded from RCSB and CheBI databases. These files were then prepared for docking using Autodock tools (version 1.5.7) (Huey, Morris, & Forli, 2012) by repairing the missing atoms, removing water, adding polar hydrogens and kolmann (for receptor) or Gasteiger charges (for ligand), creation of configuration file and grid preparation. All the structure files were then exported as.pdbqt files to be uploaded to CB-Dock2 server (20 cavity search), and Autodock Qvina for blind docking. The outputs were viewed and captured using PyMOL 2 (Schrödinger & DeLano, 2020). Autodock vina works on hybrid scoring based on the X-Score function while CB-dock server is based on curvature-based cavity detection (cavities on proteins based on clustering of solvent-accessible surface) followed by vina-based molecular docking procedure. The results were ranked on basis of the potential binding sites of the query ligand according to the Vina score (kcal/mol).

2.7. Prototype of multi-layer gelation

Two methods were used to prototype curdlan-pea protein gels' capability to generate an heterogenous structure. The white layer was made from C4P4 suspension (4% curdlan gum and 4% pea protein isolate). The same formulation (C4P4) suspension was dyed to orange by food-grade colorant (Dr. Oetker Queen Australia, Qld, Australia) to visualised the layers from different heating temperatures or durations. In the first method, approximately 20 mL of suspensions were added into a plastic cup (150 mL volume), sealed with a cap, and then heated at 80 °C for 5 min using water bath (model SWB20D, Ratek Instruments, Australia). Then each additional layer was added followed by another 5-min heating at 80 °C. In the second method, the orange layers were gelled individually at 80 °C for 5 min using the water bath. Then the C4P4 suspension was added on top of the orange layer, which was heated at 60 °C for 5 min.

2.8. Statistics

All the measurements in this study were in triplicate. The results are reported as average ± standard deviation. ANOVA was labelled as superscript of the data using SPSS (version 26.0, IBM Corp., Armonk, NY) with significant difference ($p \leq 0.05$) determined by Duncan's test. All figures were prepared using Origin (version 2019b, OriginLab Corporation, US).

3. Results and discussions

3.1. Gelling behaviours at different temperatures

Both temperature and formulation have significant impact on the gelling behaviour. To analyse the impact of temperature and isothermal duration, we start with one formulation of 4% curdlan – 4% pea protein suspension (C4P4).

3.1.1. Gelation process of curdlan-pea protein suspensions

The gelation process of curdlan-pea protein suspensions showed significant differences at different temperatures, as shown in Fig. 1. During heating, the storage modulus (G') increases steadily at first, before experiencing a sharp rise (approximately one log increase in modulus value) between 55 and 60 °C (Fig. 1A). The increasing stiffness follows: $G' \sim Te^{2\beta T}$ with thermal coefficient $\beta = 0.021$ K^{-1} within 25–50 °C which increased to $\beta = 0.118$ K^{-1} within 55–60 °C (Schoenmakers, Rowan, & Kouwer, 2018). The loss modulus (G'') showed similar trend as G' with lower modulus value than G' both in heating and cooling (Fig. 2B), which is confirmed by the tan delta values lower than 1 (Fig. 1C). Incubation at the same temperature will further increase the modulus value, and the gelation processes will finish within 1 h at 60–80 °C, while the gelation continued after 1 h at 50–55 °C (Fig. 1D). It worth to mention that further increase in heating/incubation temperatures above 60 °C does not lead to higher storage/loss modulus for curdlan-pea protein gels upon cooling (Fig. 1A&B). But the gelation continues into the cooling stage for 50/55 °C samples as indicated by the increased modulus (Fig. 1A&B). To summarise, the gelation of curdlan-pea protein could happen in a wide temperature range and may take more than 1 h to finish depending on the heating temperature.

As shown in Fig. 1E, the curdlan-pea protein suspension was able to form gels at 70–80 °C after 5 min of heating, but was unable to gel at 50–55 °C. Although similar G' was observed for gels at 60–80 °C after 5 min incubation (green line in Fig. 1D), only weak gels were formed after 5 min of heating at 60 °C, which is similar in consistency to heating at 55 °C for 60 min, indicating that there might be different gel microstructure at 60–80 °C, as discussed in the next section. The curdlan-pea protein suspension was able to form stable gels when heated above 60 °C for 60 min.

The crossover point of storage and loss modulus can indicate the sol-gel transition. No visible crossover between G' and G'' was observed at 5 °C/min without isothermal incubation (Fig. S1). Therefore, multiple waveform rheology, which may be more effective to detect the crossover point than the conventional gelling method (Seighalani, McMahon, & Sharma, 2021), was used to investigate precisely at what temperature the curdlan-pea protein suspension gelation occurs (Fig. S2). At heating rate of 1 °C/min, no significant crossover of storage and loss modulus was found in both mixture and pure curdlan at all frequencies. The difference is that the storage modulus is significantly higher than the loss modulus, around 40 °C for curdlan-pea protein suspension, while this would only occur at around 55 °C for pure curdlan.

3.1.2. Rheological properties of curdlan-pea protein gels

The results of the SAOS frequency sweep show that the gels at all temperatures exhibit similar degrees of frequency dependence. The storage modulus increases slightly with increasing angular frequency (Fig. S3A), while the complex viscosity decreases with increasing

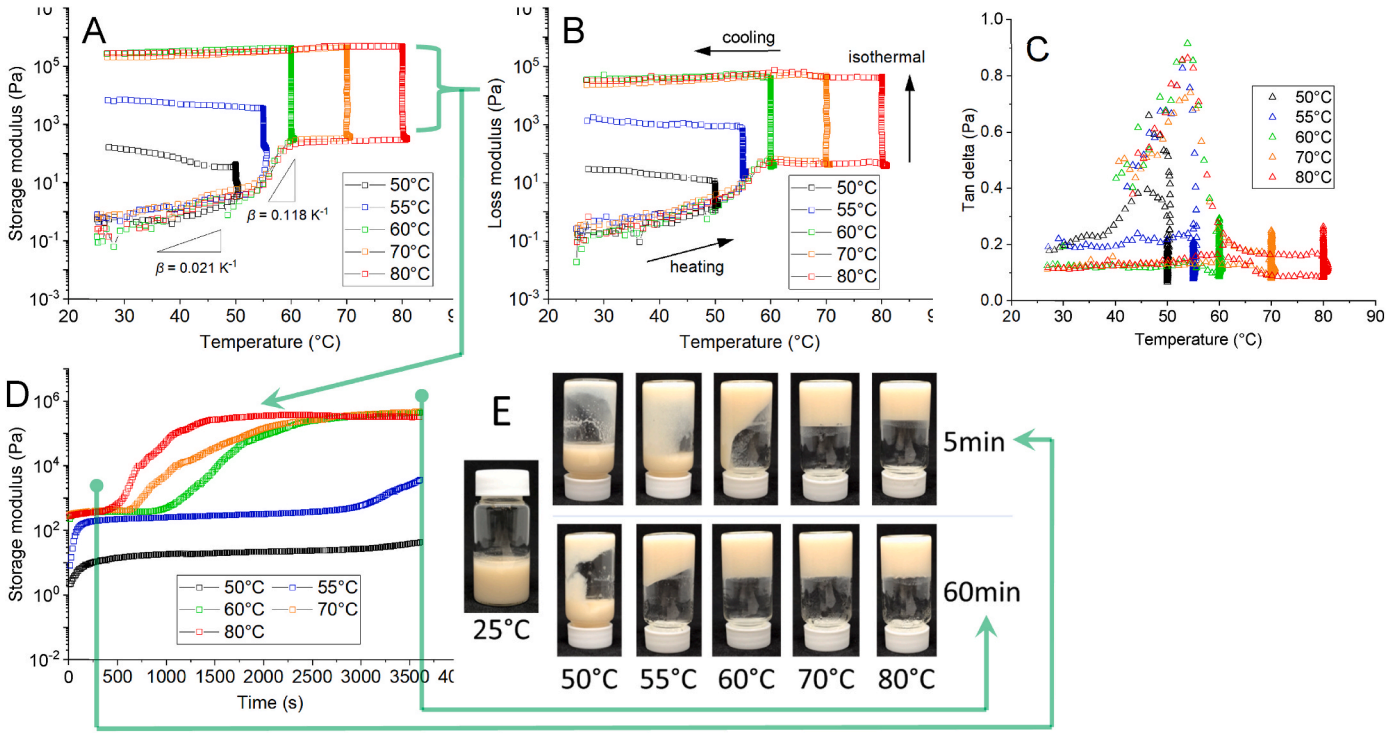

Fig. 1. Effects of heating temperatures on the gelling behaviour of curdlan gum (4% w/w) – pea protein (4% w/w) gels: A. storage modulus (inserted black triangle represent the slope of storage modulus onset between 35-50 °C and 55–60 °C, respectively); B. loss modulus (black arrows showing the thermal history of samples including heating, isothermal, and cooling stages); C. tan delta; D: curdlan gum – pea protein gels formed at different temperature and heating duration (i.e. the isothermal stage at 50/55/60/70/80 °C in sub-figure A, plotted against stage time to show the structure formation); E: appearance of gels formed at different temperatures after 5 and 60 min, respectively (green arrows show the position of storage modulus in sub-figure D at the time when these pictures were taken).

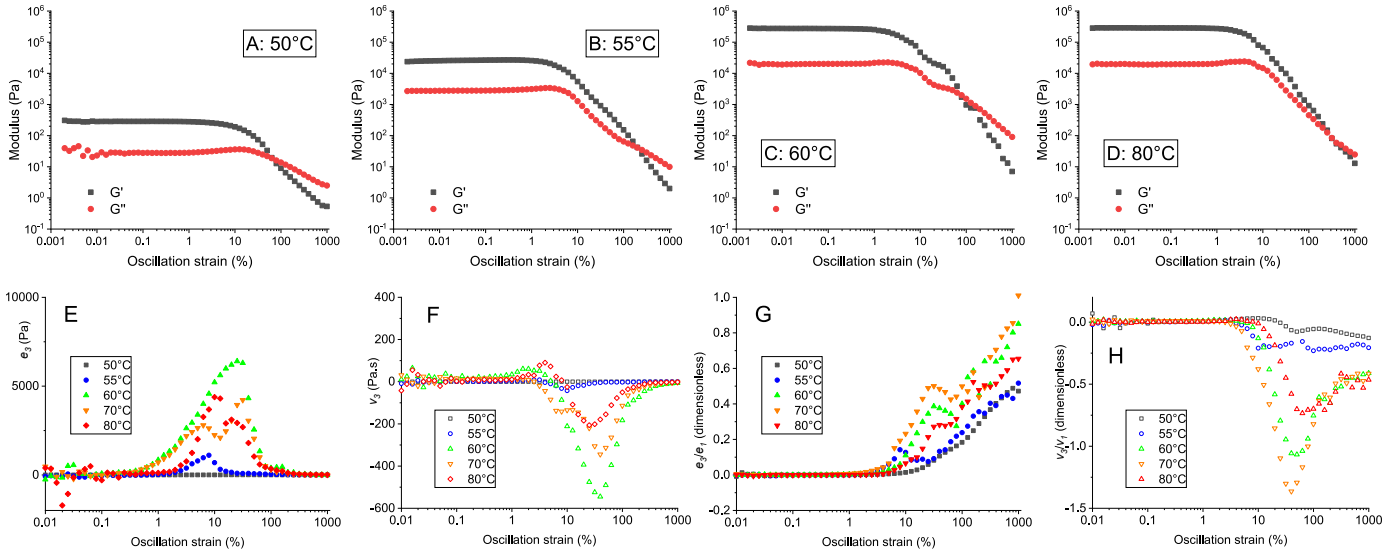

Fig. 2. Strain sweep curves of curdlan gum (4% w/w) – pea protein (4% w/w) gels in LAOS regime gelled at different temperature (A/B/C/D: 50/55/60/80 °C); Higher harmonics intensity (E/F: e_3 and v_3, G/H: e_3/e_1 and v_3/v_1) in LAOS; elastic and viscous Lissajous curve of corresponding gels (I); CLSM pictures (J) of mixture gels formed at different temperature (all scale bars represent 20 μm); and SEM pictures of mixture gels (K1–K4, green highlights show possible locations of pea protein, all scale bars represent 200 μm).

angular frequency (Fig. S3C). This indicates that the storage and loss moduli do not have strong frequency dependence, which is similar to the results reported in the literature for this type of gel (L. Zhang, Yue, Qian, & Ding, 2020). As the temperature increases from 50 to 60 °C, both storage and loss moduli increase significantly, however, the change in moduli is not significant as the temperature continues to increase to 80 °C. Based on these results, we can conclude that the mechanical properties of the gels are relatively insensitive to changes in temperature above 60 °C.

LAOS rheology can show more information on the texture of curdlan-pea protein gel at different temperatures. Storage modulus of gels formed at all temperatures maintain stable until approximately 2%

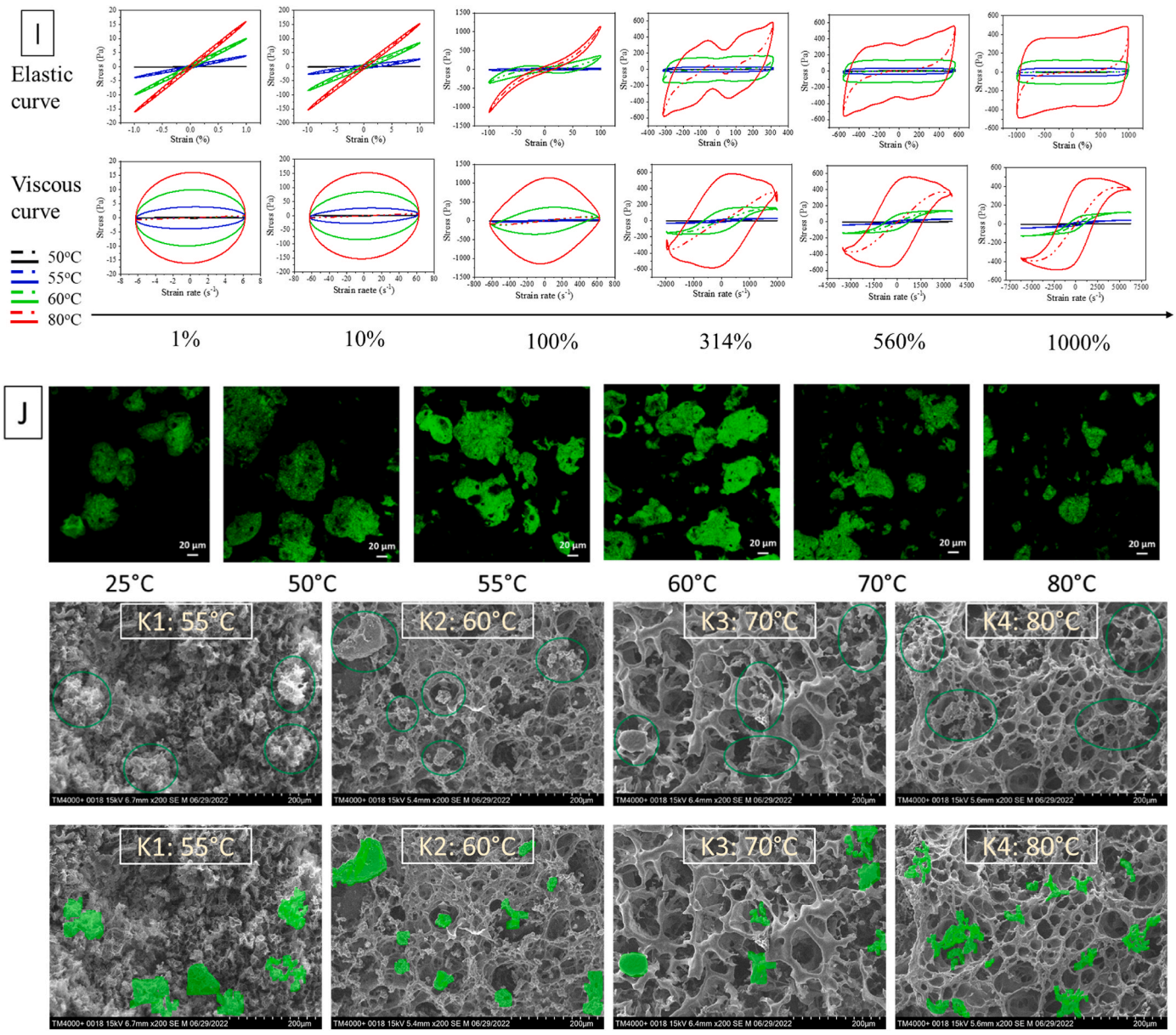

Fig. 2. (*continued*).

strain before decreasing (Fig. 2A–D), while the loss modulus shows overshot near 10% strain. Therefore all the gels can be categorized as *Type III* Weak Strain Overshot in large amplitude deformation (Hyun et al., 2011), with a slight overshoot (slight increase in the loss modulus between 1% and 100% in current study) with the increase of strain. This type of weak overshot is associated with plasticity and yielding in soft materials due to a continuous transition from recoverable to unrecoverable acquisition of strain (Donley, Singh, Shetty, & Rogers, 2020). Although the modulus values are almost identical for the gels formed at 60 or 80 °C, the crossover point of G' and G'' appears at higher strain for the 80 °C gel (316% strain for 80 °C, 79% strain for 60 °C gel, in Fig. 2C&D). It indicates that the 80 °C gel can maintain the solid-like texture during higher amplitude of mechanical deformation than the 60 °C gel (J. Yu, Wang, Li, & Wang, 2022). Extent of nonlinear viscoelastic behaviour is measured using ratio of the third harmonic viscoelastic modulus, in Fig. 2E–H. A local peak in e_3 is observed at 10%–30% strain when the heating temperature is higher than 55 °C, with the corresponding negative v_3 around similar strain amplitude, which shows the highest contribution from the third harmonics (Sousa & Gonçalves, 2015). Higher strain-stiffening behaviour was observed from 60 to 80 °C gels compared to 50–55 °C gels, because dense gel network at 60–80 °C provides more robust resistance to the large deformation (Ma, Su, Wang, Li, & Wang, 2020). All gels show nonlinear viscoelastic behaviours with the value of $e'_3/e'_1 \geq 0.01$ (Anvari & Joyner, 2018). The positive value of e'_3/e'_1 indicated the strain-stiffening from all gels despite the gelation temperatures. And the onsets of non-linearity of 60–80 °C gels take place at a lower strain, which is another proof of more strain-stiffening behaviour (Hashemnejad & Kundu, 2019).

Lissajous curves can visualise the elastic and viscous portion of the curdlan-pea protein gels at different strains and temperatures (Fig. 2I). The area covered by the Elastic Lissajous curve characterises the amount of energy stored during oscillation (Duvarci, Yazar, & Kokini, 2017). It can be seen that the gel, at all temperatures, is able to store more energy at higher strain (i.e. for the same gel as indicated by the line colour, the area covered by the elastic curves in Fig. 2I gradually increased while the strain increases from 1% to 1000%). This is also an indication of the elasticity and resistance to external deformation of the sample. At the same strain, the 80 °C gel is significantly higher in the area covered than

the other samples, especially in the large strain domain (e.g. at 1000%, the area covered by redline is larger than other lines in Fig. 2I Elastic curve). At larger strain amplitudes, the Lissajous curves for the gels exhibit squarish shapes, indicating traits of yielding behaviours (Ramya, Reddy, Shanmugam, & Deshpande, 2020). The viscous curve covers a larger area at low strain, compared to the elastic curve, and contribution of viscous properties decreases as the strain increases. This indicates that viscous is the more dominant characteristic exhibited at small strains (Schreuders et al., 2021b).

3.2. Gels morphology

Heating temperatures showed significant impact on the internal structure despite with same formulation of C4P4, as shown in Fig. 2J&K. As can be seen from the CLSM, the water absorption and swelling of PPI is significant upon heating at 50 and 55 °C (Fig. 2J), because the curdlan network formation is not yet finished at this point. And only weak interparticle connections can be observed among curdlan particles under SEM (Fig. 2K1). However, at 60 °C, the curdlan network is clearly formed with fibrous fractal structure (Fig. 2K2). As the temperature continues to rise, the skeleton of the curdlan network is more vivid, with more uniform pores and narrower fibrous structure observed in 80 °C gel (Fig. 2K4). This is because curdlan gum can form loose triple-stranded helix structure when gelled at 50–60 °C, and the helix could be partially dissociated into both double- and single-stranded chains with lower fibrous width at higher temperature such as 80–90 °C, which has been reported based on curdlan microfibrils width from atomic force microscopy by Xiao et al. (2017) and further confirmed by Gieroba et al. (2020). But the complexity of the networks as indicated by fractal dimensions of the gel backbones was not changed from 60 to 80 °C (Fig. 3C

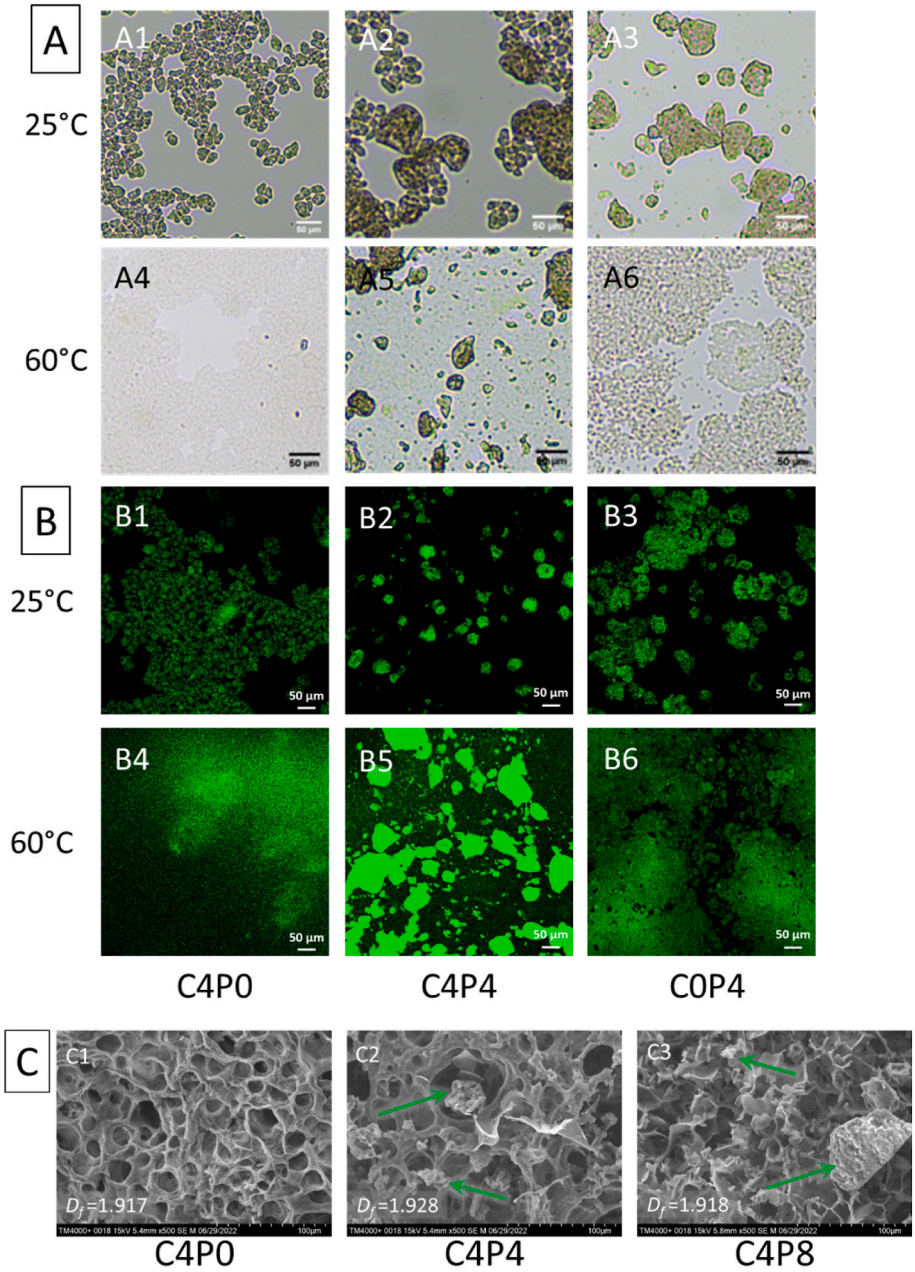

Fig. 3. Optical microscopic (A), CLSM (B), and SEM (C) pictures of curdlan gum, pea protein, and mixtures before and after gelation at 60 °C (C4: curdlan gum 4% w/w; P4: pea protein 4% w/w; both shown as green particles in B; green arrows show pea protein in C; scale bars represent 50 µm in A/B, and 100 µm in C; D_f - fractal dimension; C0P4 didn't form gel therefore not shown in SEM).

inserted values).

Curdlan gum and pea protein behave very differently upon heating. Curdlan gum is an insoluble particle in cold water (Aquinas, Bhat, & Selvaraj, 2022), suspended in water and with a clear edge (Fig. 3A1). While pea protein has low solubility in water (Q. Liu et al., 2020), it swells slightly in water (Fig. 3A3). At 25 °C there is no significant interaction between curdlan and pea protein (Fig. 3A2). After heating at 60 °C, the curdlan particles completely disappear and form the gel, which can be seen under the light microscope (Fig. 3A4) and CLSM (Fig. 3B4). The PPI particles swell when heated at 60 °C (Fig. 3A6), but unlike curdlan, pea protein still retain their granular structure, as seen via CLSM (Fig. 3B6). It should be noted that although curdlan also appears green in CLSM, they can be clearly distinguished by the difference in brightness (because curdlan required much higher laser power and fluorescence intensity than PPI to be visible in the mixture as shown in Fig. 3B5; the shape of PPI can also be confirmed by light microscope as shown in Fig. 3A5).

In the curdlan-pea protein mixture, the morphology of the pea protein differed from that of the pure protein. Although pea protein also swelled upon heating, the degree of swelling was significantly restricted compared with that of the pure protein (Fig. 3B5). This is because curdlan absorbs water more rapidly, and occupies the space for water and swelling via competitive absorption (Nishinari et al., 2021). After water absorption, curdlan incorporates the pea protein into the polysaccharide network, which can be observed in the SEM (Fig. 3C2). The network of pure curdlan consists nearly uniform distribution of pores, and a homogeneous three-dimensional network. In C4P4, pea protein particles are clearly visible in two forms. In one case, these particles are fully embedded in the curdlan network, which can be categorized as an inclusion with interparticle interactions (Shewan & Stokes, 2019); in the other case, they are partially embedded or attached to the network structure. As the pea protein itself (C0P4) cannot be gelled upon heating, only the SEM photograph of C4P8 is attached here to show the changes in the case of more pea protein addition, which shows a similar structure as C4P4 with more pea protein particles. Some of the networks can be seen to be interrupted by the existence of pea protein particles (green arrows in Fig. 3C). Moreover, changes in the structure of the curdlan network is also observed in C4P4 in that the curdlan fibres are thicker than pure curdlan (the average widths of curdlan fibres are 2.80 ± 0.69 μm for C4P0 and 5.59 ± 1.95 μm for C4P4 as shown in Fig. S4).

The other trend is that the pea protein shows smaller particle sizes at 70/80 °C. One reason for this is that the curdlan network forms rapidly, limiting the hydration swelling of the pea protein (Wu et al., 2015), as reported previously. On the other hand, it may be that the pea protein is partially cooked at higher temperatures, leading to a reduction in particle size. Smaller pea protein particles are more integrated in the curdlan network at 80 °C than at 60 °C (green area highlighted in Fig. 2K4) (Dickinson, 2012). Moreover, the particle size of pea protein can be expected to decrease further via mechanical treatment, such as homogenisation, to increase the homogeneity of the gel if needed (Su, Zhu, Wang, Li, & Wang, 2019; Wang, Sun, Li, Adhikari, & Li, 2018).

The rheology and morphology results show that we should be able to accurately tailor the gel stiffness and microstructure, not by changing the gel formulation, but rather by fine-tuning its thermal history. Selective interactions between curdlan and pea protein is a crucial step in making biomimetic networks with a controlled architecture (Schoenmakers et al., 2018).

3.3. Gelling behaviours at different protein concentrations

The effect of different pea protein concentrations on the texture of the mixed gels is more prominent in the heating phase than in the cooling phase. When heated, the modulus of mixture samples is higher than that of a pure curdlan sample (Fig. 4A&B). This is because the pea protein swells after hydration and already occupies space, therefore, curdlan molecules are more likely to form links with each other due to the volume exclusion effect from the pea protein particles (Mi et al., 2021a). During cooling (without isothermal stage), adding pea protein also results in an increase in modulus, but to a lesser extent as compared with the heating stage.

Similarly, all the nonlinear viscoelastic parameters gradually increase with the increased protein concentration (Table S1). However, no significant difference was observed in large strain modulus (G'_L) in the typical SAOS (0.1% strain) or MAOS (10% strain) range. It only shows significant differences in G'_L at 1000% strain (LAOS) when varying protein concentration, which implies that the capacity of stretching the gel network allowed the material to hold its structure at large deformations (Duvarci et al., 2017). Moreover, curdlan-pea protein gels show strain-hardening behaviours ($G'_L/G'_M > 1.10$) at strain of 1000% (Anvari & Joyner, 2018). Protein concentration also shows significant impacts on η'_L and η'_M in both SAOS and LAOS ranges in similar manner.

When isothermal stage is included, the modulus value may slightly decrease at high pea protein concentration (e.g. 8% w/w), as shown in Fig. S5A&B. Such a high amount of pea protein particles may interrupt the formation of the network structure of curdlan (as seen in Fig. 3C3). Although this difference in modulus remained the same in the strain sweep (Fig. S5C&D), no significant trend was found following the increase of protein concentrations. As shown in Fig. S5E&F, curdlan has a peak of e3 around 20% strain and the addition of pea protein causes the peak move to lower strain of around 10%. Comparison of the pure pea protein sample (Fig. S5C&D) further confirms that the pea protein particles themselves do not swell enough to form a gel of sufficient strength, and need to be embedded in the curdlan network (the pea protein heating and cooling process can be seen in Fig. 5A&B). This supports our hypothesis that the origin of both the linear and the nonlinear elasticity of the network is predominantly due to curdlan cross-linking, and the role of pea protein particles in nonlinear viscoelasticity can be modulated via their thermal history, especially the heating temperature and duration (Gardel et al., 2004).

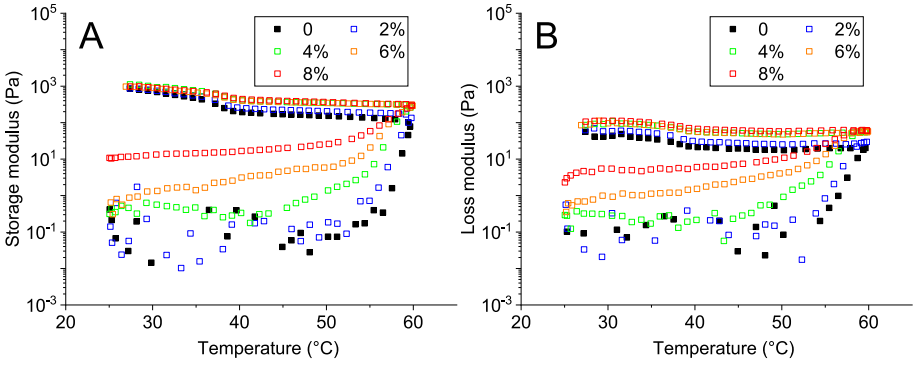

Fig. 4. Heating and cooling of curdlan-pea protein suspension at different protein concentration without isothermal stage (A: storage modulus; B: loss modulus).

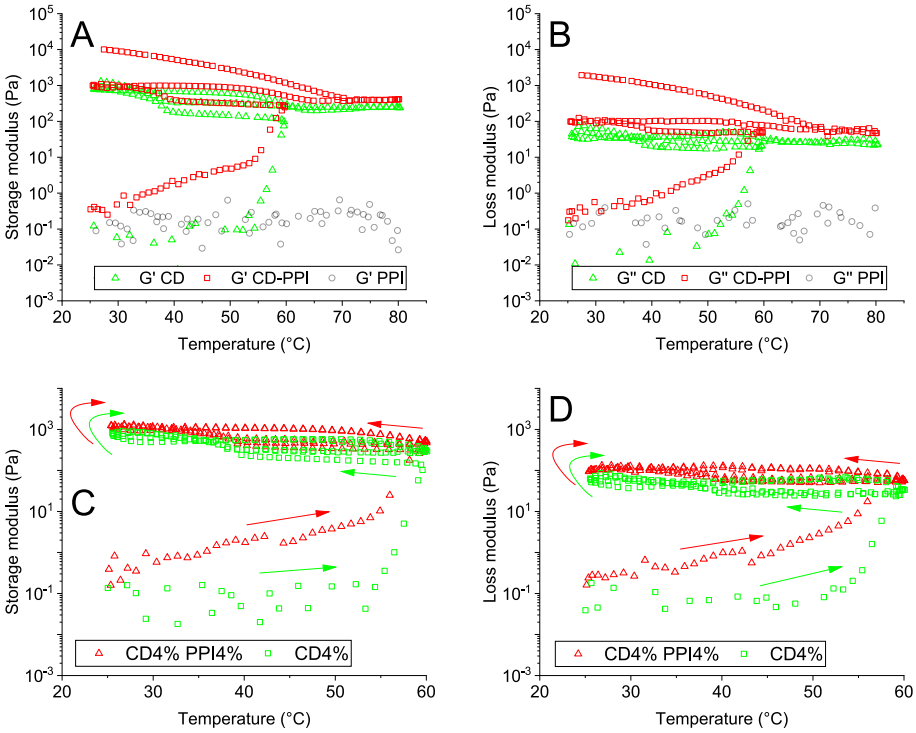

Fig. 5. Different heating pattern and incorporation of pea protein can determine the gel strength (A/B: heat to 60 °C, cool down to 25 °C, then re-heat to 80 °C, without incubation; C/D: heat/re-heat up to 60 °C without incubation) (CD, curdlan gum; PPI, pea protein isolate); Prototype of inhomogeneous structure using curdlan gum (4% w/w) – pea protein (4% w/w) gels (E: Layer-by-layer gelled continuously at 80 °C; F: Pre-gelled orange layers at 80 °C and then white layers gelled at 60 °C); diagram of curdlan-pea protein gelling behaviours at different temperature/time (G).

3.4. Layer-by-layer heterogeneous structure

It has been widely reported that curdlan gum can form a thermally reversible gel at 55–60 °C, and a thermally irreversible gel when temperature is higher than 80 °C (Tao et al., 2021). The curdlan and the mixture gels show no significant changes in modulus during the re-heating up to 60 °C (Fig. 5C&D), as indicated by the final modulus values after the initial heating and re-heating (the modulus values after first/second/third heating-cooling circles were shown in Fig. S2C&D). And the sol-gel transition as indicated by $G' > G''$ is not observed with the curdlan gum during re-heating in this study especially when pea protein is added (Qu et al., 2021), which is also confirmed by multiple waveform measurement in Fig. S2A&B. However, when gelled at 60 °C and then re-heated to 80 °C (Fig. 5A&B), both G' and G'' increase for approximately one-log (10 times higher) after 80 °C re-heating for curdlan-pea protein gels, while G' and G'' of pure curdlan gel remains at the same level before and after re-heating at 80 °C.

A diagram is used to illustrate the effects of thermal history combining heating temperature and isothermal duration on curdlan-pea protein gels in Fig. 5E. In general, rigid and dense gel network can be formed at higher temperatures, and the gelation will finish earlier at higher temperatures. Four typical gels were selected in the diagram to compare. Gel I is formed at high temperatures within short periods, which represents both the orange or white layers in the layer-by-layer method in Fig. 5F. Gel II, formed at high temperatures over long periods, represents the orange layer in Fig. 5G to achieve high modulus and dense gel network. The white layer in Fig. 5G was shown as Gel III, which provides soft texture that is different from the orange layer. Moreover, when Gel III was further heated at 80 °C, it can turn into Gel IV with significant higher modulus as confirmed in Fig. 5A&B. Therefore, the gels can be fixed in shape at low temperatures (Gel III) and the gel strength can then be reinforced in selected area by further heating (Gel IV) to create inhomogeneous structures.

The unique gelling behaviour of curdlan-pea protein mixture makes it possible to build heterogeneous structures by modulating their thermal history. We demonstrated it by prototyping such structure using two different heating methods. The first is the formation of a gel by layer-by-layer at 80 °C only (Fig. 5F). This gel can be tightly bonded between the different coloured layers, if the next layer of suspension is added just as the previous gel is being formed (approximately 5 min for 4% curdlan – 4% pea protein gels). The second type is to finish the gelation of orange part at 80 °C until the modulus enters stable plateau (approximately 1 h based on Fig. 1D), and then the white layer at 60 °C to re-combine the orange layers, as shown in Fig. 5G. The advantage of the second gel is that it forms a tightly bound gel while maintaining different structures (Fig. 2K4 compared to Fig. 2K2) and different viscoelasticity between the orange and white layers.

3.5. Gelling mechanism of curdlan-pea protein gels

The gelling mechanisms of curdlan gel differ with or without pea protein addition (Fig. 6A). Without protein, curdlan gum can form 3-D fibrous gel network (Fig. 3C1) and uniform hollow areas, as illustrated in Fig. 6A1. The gelation of curdlan gum is achieved by cross-linking of the β-glucan molecules (Fig. 6A5) (Aquinas et al., 2022; Tao et al., 2021). Taking into account the chemical structure of curdlan, the gelation of native curdlan should be attributed to hydrogen bonding along with hydrophobic interaction (Cai & Zhang, 2017). On the contrary, pea protein particles will not form gels but only swell into larger pieces (Fig. 3A6 & B6) upon heating and hydration as shown in Fig. 6A2.

When curdlan-pea protein mixture gelled at 60 °C, the pea protein particles also swell and can partially embed into the curdlan gel network (Fig. 6A3). The fibrous structure of curdlan gum also becomes thicker in the presence of pea protein, with increased average fibre width as shown in Fig. S5. Compared with pure pea protein, the swelling of protein particles is restrained (Fig. 3B5 vs. B6) by both the physical barrier of

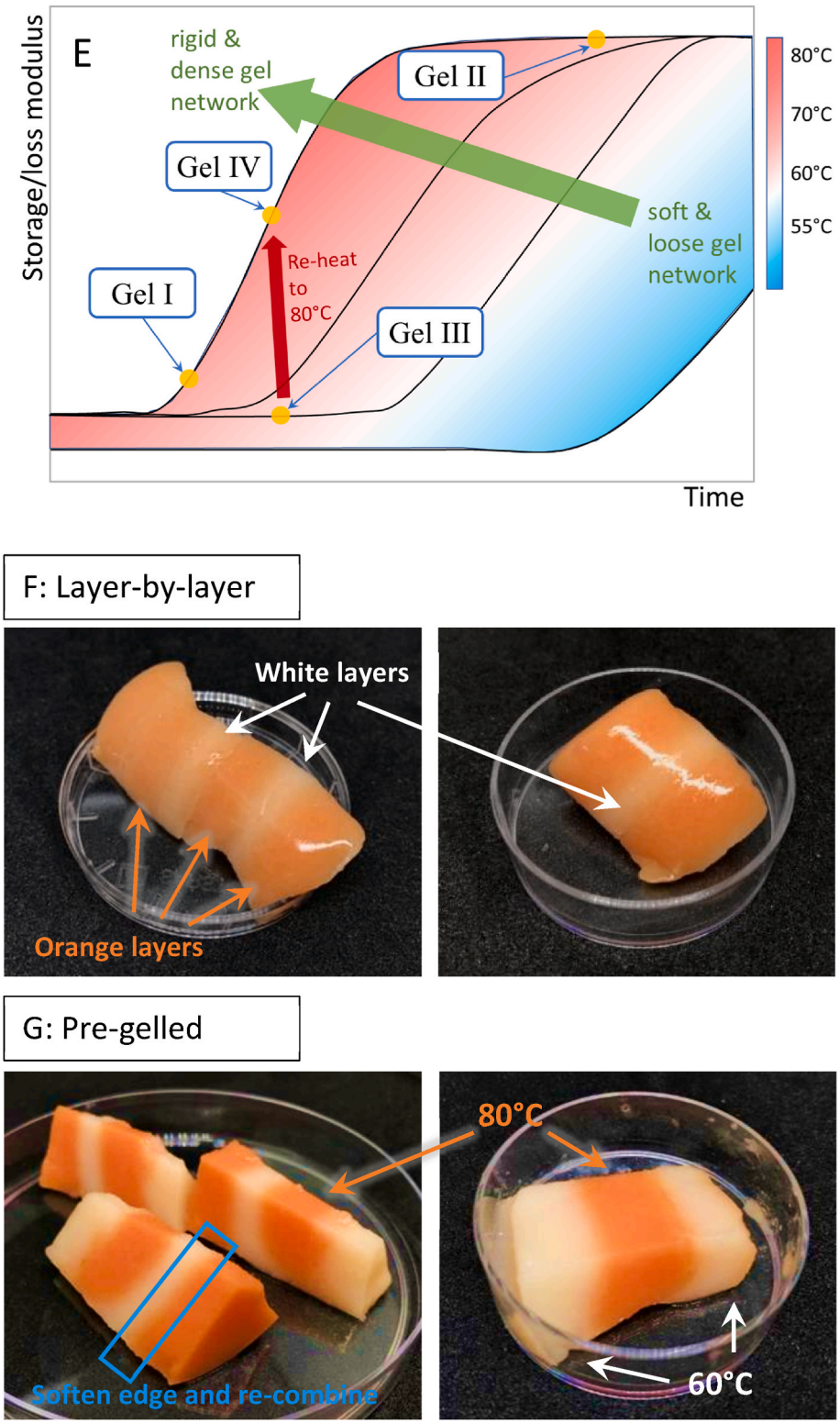

Fig. 5. (*continued*).

curdlan network and the competition in absorbing water. As gelling temperature rises to 80 °C as shown in Fig. 6A4, curdlan-pea protein mixture forms a gel with dense network and narrow fibrous structure that is similar in fibre width to pure curdlan gel (Fig. S5B). The pea protein particles that initially are dispersed in a liquid-like suspension, and upon heating and aggregation, become arrested in space-spanning structures in the curdlan gel network that make the substance rigid. Moreover, the protein particles not only decrease in size, but also fully merge into the curdlan network (Fig. 2K4). The fully merged protein particles in the gel network are similar topologically to the animal tissue cells that interlinked by extracellular matrix, which shows the potential to mimic the mechanical response upon deformation (van Oosten et al., 2019).

The FT-IR spectra, a useful tool to analyse possible interactions

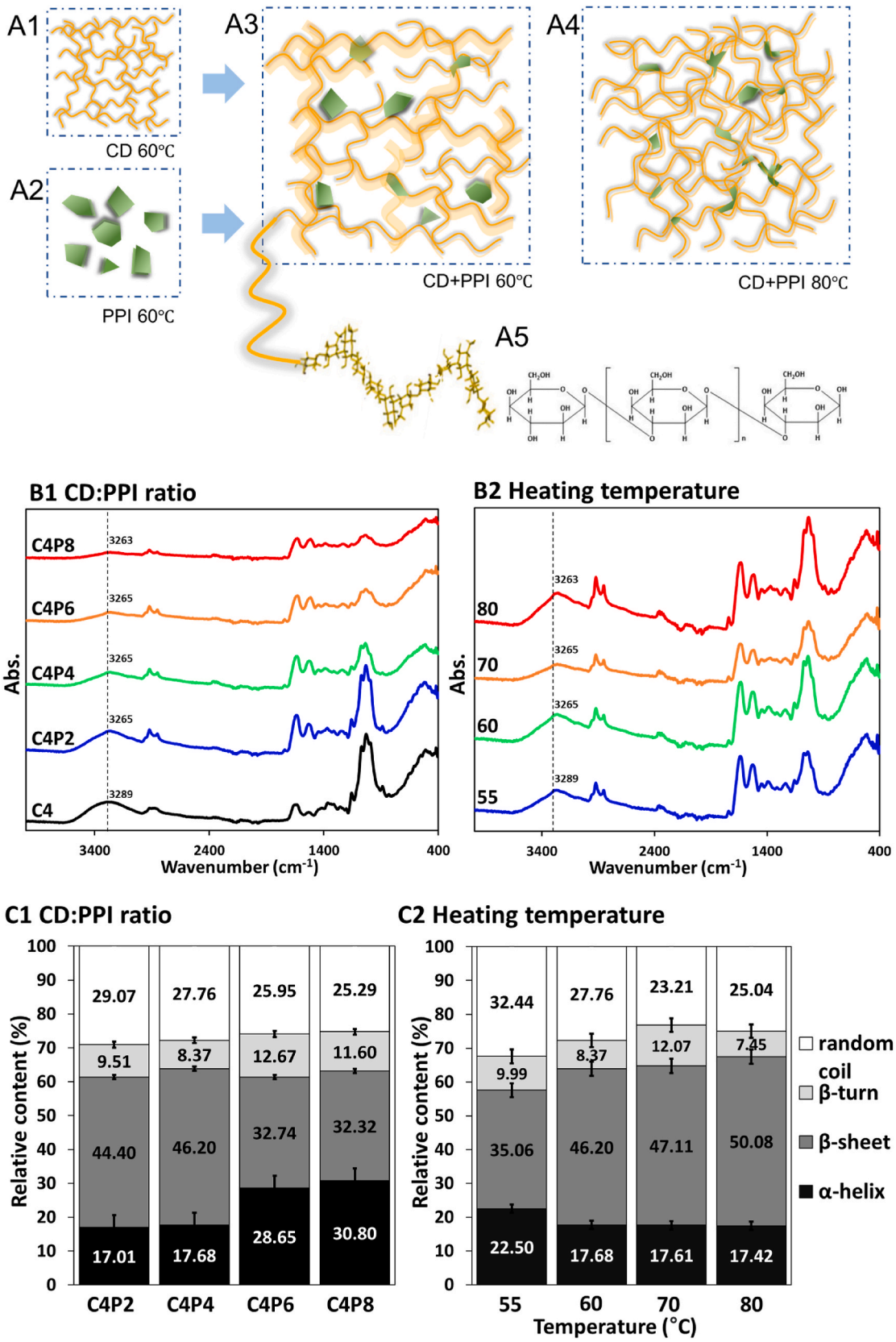

Fig. 6. Proposed gelling mechanism of curdlan gel (A1), pea protein (A2), curdlan-pea protein gels at 60 or 80 °C (A3&A4), single helix curdlan (adopted from Tao et al. (2021) with permission) and chemical structure of curdlan (adopted from Aquinas et al. (2022) with permission) (A5); FTIR spectrum of gels with different protein concentration and temperature (B1/2), protein secondary structure (C1/2).

between pea protein and curdlan gum, show several peaks including 3289 cm^{-1} (Amide band A, N–H or O–H stretching vibration peak), 1652 cm^{-1} (Amide band I, C═O and C═N stretching), 1540 cm^{-1} (Amide bend II, C–N stretching vibration), and 1069 cm^{-1} (C–O stretching vibration) (Fig. 6B1&2) (Q. Li et al., 2019). The intensity of C–O stretching vibration peak around 1069 cm^{-1} decreases with increasing the amount of pea protein. The addition of pea protein and increasing heating temperature did not induce a new peak formation, indicating no chemical reactions between pea protein and curdlan gum during heating. The amide band A shifted from 3289 cm^{-1} to 3265 cm^{-1} according to increasing the amount of pea protein and the heating temperature, suggesting that hydrogen bonding between pea protein and curdlan gum was promoted (hydrogen bonding is also predicted as the primary interaction between pea protein and curdlan gum from molecular docking simulation as shown in Fig. S7 and Table S2), and the similar patterns were observed in previous literatures (M. Li et al., 2022b; Q. Li et al., 2019; Yu et al., 2022).

The relative secondary structure content estimated by analysing Amide Iband showed a significant difference between samples according to the pea protein/curdlan gum ratio and heating temperature (Fig. 6C1&2). With increasing heating temperature, a decrease in α-helix and an increase in β-sheet were observed. Generally, the formation of β-sheet is caused by the unfolding of a-helix during heat-induced gelation, indicating the unfolded protein exposes the hydrophobic sites to interact with polysaccharide (Mi et al., 2021b). Previous studies also found a decrease of a-helix content and an increase of β-sheet content due to the protein and polysaccharide interaction during heating process, which is beneficial for gel formation (Zhou et al., 2019). In addition, the lower a-helix content and the higher β-sheet content were found when the smaller amount of pea protein was added, indicating unfolding of pea protein were promoted by curdlan gum, and this phenomenon has been found in previous studies (J. Chen et al., 2020; Shuai Jiang et al., 2020; Mi et al., 2021b).

4. Conclusions

The unique role of temperature in regulating the texture of curdlan gum-pea protein hybrid gels was identified in this study. In the range of 55–60 °C, the curdlan-pea protein suspension formed weak gel. As the temperature increases to 80 °C, the mixed gel becomes thermally irreversible, and the storage/loss modulus of the gel increases significantly. When small amounts of pea protein are added (2–4%), the gels still form a continuous gel network. However, when the pea protein concentration was increased to 8%, the gel network was partially separated by particles of pea protein and resulting in a slight decrease in the storage/loss modulus. As shown in the CLSM and SEM images, pea protein can be partially embedded in the three-dimensional structure of the gel (60 °C) or wholly embedded in the gel (80 °C), highlighting the important role of gel temperature in controlling the structural and rheological properties of curdlan-pea protein gels.

Using gel characteristics at different temperatures and formulations, it is possible to construct heterogeneous/mixed structures containing plant proteins in curdlan-pea protein gel. Layers gelled at 80 °C have a higher storage modulus than 60 °C layers (approximately by an order of magnitude). Moreover, the layers formed at different temperatures can be tightly merged. This new gelling technique could also be applied in texturizing heterogeneous structure using other plant proteins which cannot form firm solid-like texture by themselves, and in creating plant-based meat alternative products with heterogeneous structure.

Credit author statement

Yong Wang: Conceptualization; Data curation; Formal analysis; Investigation; Methodology; Visualization; Roles/Writing - original draft. Woojoeng Kim: Data curation; Visualization; Roles/Writing - original draft. Rishi Ravindra Naik: Data curation; Visualization; Roles/Writing - original draft. Patrick T. Spicer: Methodology, Writing - review & editing. Cordelia Selomulya: Conceptualization; Funding acquisition; Methodology; Project administration; Resources; Supervision; Writing - review & editing.

Declaration of competing interest

None.

Data availability

Data will be made available on request.

Acknowledgement

The installation of TA ARES G2 rheometer at UNSW Sydney is supported by the UNSW Research Infrastructure Scheme (RIS) grant scheme. The authors acknowledge the support from ARC DP200100642 (Selomulya et al.).

Appendix A. Supplementary data

Supplementary data to this article can be found online at https://doi.org/10.1016/j.foodhyd.2023.108611.

References

Alhossary, A., Handoko, S. D., Mu, Y., & Kwoh, C.-K. (2015). Fast, accurate, and reliable molecular docking with QuickVina 2. *Bioinformatics, 31*(13), 2214–2216.
Anvari, M., & Joyner, H. S. (2018). Effect of fish gelatin and gum Arabic interactions on concentrated emulsion large amplitude oscillatory shear behavior and tribological properties. *Food Hydrocolloids, 79*, 518–525.
von Braun, J., Afsana, K., Fresco, L. O., & Hassan, M. (2021). Food systems: Seven priorities to end hunger and protect the planet. *Nature, 597*(7874), 28–30.
Aquinas, N., Bhat, M. R., & Selvaraj, S. (2022). A review presenting production, characterization, and applications of biopolymer curdlan in food and pharmaceutical sectors. *Polymer Bulletin, 79*(9), 6905–6927.
Cai, Z., & Zhang, H. (2017). Recent progress on curdlan provided by functionalization strategies. *Food Hydrocolloids, 68*, 128–135.
Chen, D., & Campanella, O. H. (2022). Limited enzymatic hydrolysis induced pea protein gelation at low protein concentration with less heat requirement. *Food Hydrocolloids, 128*.
Chen, J., Deng, T., Wang, C., Mi, H., Yi, S., Li, X., et al. (2020). *Effect of hydrocolloids on gel properties and protein secondary structure of silver carp surimi, 100* pp. 2252–2260). J. J. o. t. S. o. F., & Agriculture, 5.
Chen, Q. L., Zhang, J. C., Zhang, Y. J., Meng, S., & Wang, Q. (2021). Rheological properties of pea protein isolate-amylose/amylopectin mixtures and the application in the high-moisture extruded meat substitutes. *Food Hydrocolloids, 117*.
Dickinson, E. (2012). Emulsion gels: The structuring of soft solids with protein-stabilized oil droplets. *Food Hydrocolloids, 28*(1), 224–241.
Donley, G. J., Singh, P. K., Shetty, A., & Rogers, S. A. (2020). Elucidating the G'' overshoot in soft materials with a yield transition via a time-resolved experimental strain decomposition. *Proceedings of the National Academy of Sciences of the United States of America, 117*(36), 21945–21952.
Duvarci, O. C., Yazar, G., & Kokini, J. L. (2017). The comparison of Laos behavior of structured food materials (suspensions, emulsions and elastic networks). *Trends in Food Science & Technology, 60*, 2–11.
Florczuk, A., Dąbrowska, A., & Aljewicz, M. (2022). An evaluation of the effect of curdlan and scleroglucan on the functional properties of low-fat processed cheese spreads. *Lebensmittel-Wissenschaft & Technologie, 163*.
Freeman, R., Han, M., Alvarez, Z., Lewis, J. A., Wester, J. R., Stephanopoulos, N., et al. (2018). Reversible self-assembly of superstructured networks. *Science, 362*(6416), 808–+.
Gardel, M. L., Shin, J. H., MacKintosh, F. C., Mahadevan, L., Matsudaira, P., & Weitz, D. A. (2004). Elastic Behavior of cross-linked and bundled actin networks. *Science, 304*(5675), 1301–1305.
Gieroba, B., Sroka-Bartnicka, A., Kazimierczak, P., Kalisz, G., Pieta, I. S., Nowakowski, R., et al. (2020). Effect of gelation temperature on the molecular structure and physicochemical properties of the curdlan matrix: Spectroscopic and microscopic analyses. *International Journal of Molecular Sciences, 21*(17).
Hashemnejad, S. M., & Kundu, S. (2019). Rheological properties and failure of alginate hydrogels with ionic and covalent crosslinks. *Soft Matter, 15*(39), 7852–7862.
Huey, R., Morris, G. M., & Forli, S. (2012). *Using AutoDock 4 and AutoDock vina with AutoDockTools: A tutorial, 10550*. The Scripps Research Institute Molecular Graphics Laboratory, Article 92037.
Hyun, K., Wilhelm, M., Klein, C. O., Cho, K. S., Nam, J. G., Ahn, K. H., et al. (2011). A review of nonlinear oscillatory shear tests: Analysis and application of large amplitude oscillatory shear (Laos). *Progress in Polymer Science, 36*(12), 1697–1753.

Jiang, S., Cao, C. A., Xia, X. F., Liu, Q., & Kong, B. H. (2019). Enhancement of the textural and gel properties of frankfurters by adding thermo-reversible or thermo-irreversible curdlan gels. *Journal of Food Science, 84*(5), 1068–1077.

Jiang, S., Zhao, S., Jia, X., Wang, H., Zhang, H., Liu, Q., et al. (2020). *Thermal gelling properties and structural properties of myofibrillar protein including thermo-reversible and thermo-irreversible curdlan gels, 311*, Article 126018.

Kim, W., Wang, Y., & Selomulya, C. (2020). Dairy and plant proteins as natural food emulsifiers. *Trends in Food Science & Technology, 105*, 261–272.

Kornet, R., Veenemans, J., Venema, P., van der Goot, A. J., Meinders, M., Sagis, L., et al. (2021). Less is more: Limited fractionation yields stronger gels for pea proteins. *Food Hydrocolloids, 112*.

Liu, Q., Dai, Y., Hou, H., Wang, W., Ding, X., Zhang, H., et al. (2020). Changes in the structure and emulsification properties of pea protein isolate during grinding. *Lebensmittel-Wissenschaft & Technologie, 133*.

Liu, Y., Yang, X., Gan, J., Chen, S., Xiao, Z.-X., & Cao, Y. (2022). CB-Dock2: Improved protein–ligand blind docking by integrating cavity detection, docking and homologous template fitting. Nucleic Acids Research, 50(W1), W159-W164.

Li, Q., Wang, P., Miao, S., Zhang, L., & Zheng, B. (2019). Curdlan enhances the structure of myosin gel model. *Food Sciences and Nutrition, 7*(6), 2123–2130.

Li, M., Yang, R., Feng, X., Fan, X., Liu, Y., Xu, X., et al. (2022a). Effects of low-frequency and high-intensity ultrasonic treatment combined with curdlan gels on the thermal gelling properties and structural properties of soy protein isolate. *Food Hydrocolloids, 127*.

Li, M., Yang, R., Feng, X., Fan, X., Liu, Y., Xu, X., et al. (2022b). *Effects of low-frequency and high-intensity ultrasonic treatment combined with curdlan gels on the thermal gelling properties and structural properties of soy protein isolate, 127*, Article 107506.

Ma, Y., Su, D., Wang, Y., Li, D., & Wang, L. (2020). Effects of concentration and NaCl on rheological behaviors of konjac glucomannan solution under large amplitude oscillatory shear (Laos). *Lebensmittel-Wissenschaft & Technologie, 128*.

Mi, H., Li, Y., Wang, C., Yi, S., Li, X., & Li, J. (2021a). The interaction of starch-gums and their effect on gel properties and protein conformation of silver carp surimi. *Food Hydrocolloids, 112*.

Mi, H., Li, Y., Wang, C., Yi, S., Li, X., & Li, J. (2021b). *The interaction of starch-gums and their effect on gel properties and protein conformation of silver carp surimi, 112*, Article 106290.

Nishinari, K., Zhang, H., & Funami, T. (2021). Chapter 29 - curdlan. In G. O. Phillips, & P. A. Williams (Eds.), *Handbook of hydrocolloids* (3rd ed., pp. 887–921). Woodhead Publishing.

van Oosten, A. S. G., Chen, X., Chin, L., Cruz, K., Patteson, A. E., Pogoda, K., et al. (2019). Emergence of tissue-like mechanics from fibrous networks confined by close-packed cells. *Nature, 573*(7772), 96–101.

Poore, J., & Nemecek, T. (2019). Reducing food's environmental impacts through producers and consumers (vol 363, eaaw9908, 2019). *Science, 363*(6430), 939, 939.

Prabha, K., Ghosh, P., S, A., Joseph, R. M., Krishnan, R., Rana, S. S., et al. (2021). Recent development, challenges, and prospects of extrusion technology. *Future Foods, 3*, Article 100019.

Qu, R., Wang, Y., Li, D., & Wang, L. (2021). The study of rheological properties and microstructure of carboxylated nanocellulose as influenced by level of carboxylation. *Food Hydrocolloids, 121*.

Ramya, K. A., Reddy, S. M. M., Shanmugam, G., & Deshpande, A. P. (2020). Fibrillar network dynamics during oscillatory rheology of supramolecular gels. *Langmuir, 36*(44), 13342–13355.

Schoenmakers, D. C., Rowan, A. E., & Kouwer, P. H. J. (2018). Crosslinking of fibrous hydrogels. *Nature Communications, 9*(1), 2172.

Schreuders, F. K. G., Sagis, L. M. C., Bodnár, I., Erni, P., Boom, R. M., & van der Goot, A. J. (2021a). Mapping the texture of plant protein blends for meat analogues. *Food Hydrocolloids, 118*.

Schreuders, F. K. G., Sagis, L. M. C., Bodnár, I., Erni, P., Boom, R. M., & van der Goot, A. J. (2021b). Small and large oscillatory shear properties of concentrated proteins. *Food Hydrocolloids, 110*.

Schrödinger, L., & DeLano, W. (2020). *PyMOL. The PyMOL molecular graphics system*. version.

Seighalani, F. Z. B., McMahon, D. J., & Sharma, P. (2021). Determination of critical gel-sol transition point of Highly Concentrated Micellar Casein Concentrate using multiple waveform rheological technique. *Food Hydrocolloids, 120*.

Seo, B. R., Chen, X., Ling, L., Song, Y. H., Shimpi, A. A., Choi, S., et al. (2020). Collagen microarchitecture mechanically controls myofibroblast differentiation. *Proceedings of the National Academy of Sciences, 117*(21), 11387–11398.

Sha, L., & Xiong, Y. L. (2020). Plant protein-based alternatives of reconstructed meat: Science, technology, and challenges. *Trends in Food Science & Technology, 102*, 51–61.

Shewan, H., & Stokes, J. (2019). Food structure development for rheological/tribological performance. In *Handbook of food structure development* (pp. 173–198).

Sim, S. Y. J., Karwe, M. V., & Moraru, C. I. (2019). High pressure structuring of pea protein concentrates. *Journal of Food Process Engineering, 42*(7).

Sousa, A. M. M., & Gonçalves, M. P. (2015). The influence of locust bean gum on native and alkali-modified agar gels. *Food Hydrocolloids, 44*, 461–470.

Su, D., Zhu, X., Wang, Y., Li, D., & Wang, L. (2019). Effects of high-pressure homogenization on physical and thermal properties of citrus fiber. *Lebensmittel-Wissenschaft und -Technologie, 116*.

Tanger, C., Müller, M., Andlinger, D., & Kulozik, U. (2022). Influence of pH and ionic strength on the thermal gelation behaviour of pea protein. *Food Hydrocolloids, 123*.

Tang, M.-x., Lei, Y.-c., Wang, Y., Li, D., & Wang, L.-j. (2021). Rheological and structural properties of sodium caseinate as influenced by locust bean gum and κ-carrageenan. *Food Hydrocolloids, 112*.

Tao, H., Wang, B., Wen, H., Cui, B., Zhang, Z., Kong, X., et al. (2021). Improvement of the textural characteristics of curdlan gel by the formation of hydrogen bonds with erythritol. *Food Hydrocolloids, 117*.

Verma, D. K., Niamah, A. K., Patel, A. R., Thakur, M., Singh Sandhu, K., Chavez-Gonzalez, M. L., et al. (2020). Chemistry and microbial sources of curdlan with potential application and safety regulations as prebiotic in food and health. *Food Research International, 133*, Article 109136.

Wang, Y., & Selomulya, C. (2022). Food rheology applications of large amplitude oscillation shear (Laos). *Trends in Food Science & Technology, 127*, 221–244.

Wang, Y., Sun, P., Li, H., Adhikari, B., & Li, D. (2018). Rheological behavior of tomato fiber suspensions produced by high shear and high pressure homogenization and their application in tomato products. *International Journal of Analytical Chemistry*, Article 5081938, 2018.

Wei, Y., Zhang, T., Yu, F., Xue, Y., Li, Z., Wang, Y., et al. (2018). Effects of curdlan on the texture and structure of Alaska pollock surimi gels treated at 120°C. *International Journal of Food Properties, 21*(1), 1778–1788.

Willett, W., Rockström, J., Loken, B., Springmann, M., Lang, T., Vermeulen, S., et al. (2019). Food in the anthropocene: The EAT–lancet commission on healthy diets from sustainable food systems. *The Lancet, 393*(10170), 447–492.

Wu, C., Yuan, C., Chen, S., Liu, D., Ye, X., & Hu, Y. (2015). The effect of curdlan on the rheological properties of restructured ribbonfish (Trichiurus spp.) meat gel. *Food Chemistry, 179*, 222–231.

Xiao, M., Jiang, M., Wu, K., Yang, H., Ni, X., Yan, W., et al. (2017). Investigation on curdlan dissociation by heating in water. *Food Hydrocolloids, 70*, 57–64.

Yang, J., Zamani, S., Liang, L., & Chen, L. (2021). Extraction methods significantly impact pea protein composition, structure and gelling properties. *Food Hydrocolloids, 117*.

Ye, Q., Georges, N., & Selomulya, C. (2018). Microencapsulation of active ingredients in functional foods: From research stage to commercial food products. *Trends in Food Science & Technology, 78*, 167–179.

Yu, J., Wang, Y., Li, D., & Wang, L.-j. (2022). Freeze-thaw stability and rheological properties of soy protein isolate emulsion gels induced by NaCl. *Food Hydrocolloids, 123*.

Yu, J., Wang, X.-y., Li, D., Wang, L.-j., & Wang, Y. (2022). Development of soy protein isolate emulsion gels as extrusion-based 3D food printing inks: Effect of polysaccharides incorporation. *Food Hydrocolloids, 131*.

Yu, J., Wang, X.-y., Li, D., Wang, L.-j., & Wang, Y. J. F. H. (2022). *Development of soy protein isolate emulsion gels as extrusion-based 3D food printing inks: Effect of polysaccharides incorporation*, Article 107824.

Yu, P., Zhou, F., & Yang, D. (2019). Curdlan conformation change during its hydrolysis by multi-domain beta-1,3-glucanases. *Food Chemistry, 287*, 20–27.

Zhang, S., Huang, W., Feizollahi, E., Roopesh, M. S., & Chen, L. (2021). *Improvement of pea protein gelation at reduced temperature by atmospheric cold plasma and the gelling mechanism study, 67*. Innovative Food Science & Emerging Technologies.

Zhang, L., Yue, L. N., Qian, J. Y., & Ding, X. L. (2020). Effect of curdlan on the rheological properties of hydroxypropyl methylcellulose. *Foods, 10*(1).

Zhao, H., Chen, J., Hemar, Y., & Cui, B. (2020). Improvement of the rheological and textural properties of calcium sulfate-induced soy protein isolate gels by the incorporation of different polysaccharides. *Food Chemistry, 310*, Article 125983.

Zhou, X., Chen, H., Lyu, F., Lin, H., Zhang, Q., & Ding, Y. (2019). *Physicochemical properties and microstructure of fish myofibrillar protein-lipid composite gels: Effects of fat type and concentration, 90* pp. 433–442).